Japanese Journal of Applied Physics **53**, 08NG01 (2014) **REGULAR PAPER**
http://dx.doi.org/10.7567/JJAP.53.08NG01

Effects of Nb_2O_5 and SiO_2 buffer layers on the suppression of potassium out-diffusion into indium tin oxide electrode formed on chemically strengthened glass

Chan-Hwa Hong[1,3], Jae-Heon Shin[1], Nae-Man Park[1], Kyung-Hyun Kim[1], Bo-Sul Kim[1], Joon-Seop Kwak[2*], Byeong-Kwon Ju[3*], and Woo-Seok Cheong[1*]

[1]*Electronics and Telecommunication Research Institute, Daejeon 305-700, Korea*
[2]*Department of Printed Electronics Engineering, Sunchon National University, Suncheon, Jeonnam 540-742, Korea*
[3]*Display and Nanosystem Laboratory, College of Engineering, Korea University, Seoul 136-713, Korea*
E-mail: cws@etri.re.kr; bkju@korea.ac.kr; jskwak@sunchon.ac.kr

Received January 3, 2014; accepted March 15, 2014; published online July 3, 2014

We have investigated the electrical properties of indium tin oxide (ITO) thin films deposited on chemically strengthened glass (CSG) substrate by room-temperature ionized physical vapor deposition (IPVD). The ITO thin film on the CSG substrate shows a higher sheet resistance after high-temperature anneal process (>200 °C) possibly due to the out-diffusion of potassium ions (K^+) from the CSG. We have improved the electrical properties of the ITO thin film by inserting Nb_2O_5/SiO_2 buffer layers between the ITO layer and the CSG substrate. As a result, a protected and index-matched 30-nm-thick ITO thin film with sheet resistance less than 120 Ω/sq and optical transmittance higher than 90% (at 550 nm) has been achieved.

1. Introduction

Projective capacitive touch screen panels (TSPs) have been widely used due to their intuitive user interface for portable electronic devices ranging from mobile to tablet PCs.[1–5] Conventional methods for the formation of the capacitive TSP on active matrix liquid crystal display (AMLCD) and/or active matrix organic light emitting display (AMOLED) were the use of two patterned InSnO (ITO) films or a single glass having patterned ITO electrodes on both sides.[6] ITO has been widely used as a transparent conducting oxide material because of its high transmittance and low electric resistivity.[7–13] Recently, direct patterned window (DPW) technology, in which the ITO is directly deposited on chemically strengthened glass (CSG), is attracting much interest for higher optical transmittance and simple TSP processes.[1] In general, the CSG is made from soda-lime glass by a strengthening process (ion-exchange surface treatment). During the strengthening process, many potassium ions (K^+) are supplied from environment to the glass and other native ions in the glass (5–10 μm under the surface) are replaced by the potassium ions.[14,15] Therefore, the electrical properties of the ITO thin film could be deteriorated by potassium out-diffusion during high temperature heat process.[16] Hong et al. reported that the sheet resistance of an InZnO thin film deposited even on a soda-lime glass increases after heat treatment (at 150 °C) caused by the potassium out-diffusion from the glass.[17]

In this study, we have investigated the effect of buffer layers such as SiO_2 and Nb_2O_5 between the ITO layer and the CSG substrate to suppress the out-diffusion of K^+ from the CSG. As a result, a protected and index-matched 30-nm-thick ITO thin film with sheet resistance less than 120 Ω/sq and optical transmittance higher than 90% (at 550 nm) has been achieved. Moreover, the optical and electrical properties of the ITO thin film show virtually no change after humidity and thermal stress tests.

2. Experimental procedure

Depositions of SiO_2 and Nb_2O_5 films were performed in RF and DC magnetron sputtering systems, respectively. Ar-diluted O_2 gas (5%) was used for both depositions. The RF/DC powers for the SiO_2 and Nb_2O_5 depositions were 1100 and 190 W, respectively. The working pressure was 3.4 mTorr also for both depositions. Deposition of 30-nm ITO thin film was performed in room temperature in an ionized physical vapor deposition (IPVD) system, a DC magnetron sputtering system equipped with inductively coupled plasma (ICP).[18–20] Ar-diluted O_2 gas (0.4%) and an ITO target (3 wt % SnO_2-doped In_2O_3) were used for the deposition. The DC sputtering power and the ICP power for the ITO deposition were 600 and 400 W, respectively. The working pressure was 5 mTorr. After deposition of the ITO thin film, a heat treatment (25–400 °C) was carried out in a box furnace for 1 h in vacuum condition.

The sheet resistances of the ITO films were measured at room temperature by using four-point probe technique as a function of annealing temperature and of buffer layer. The optical transmittances of the samples were measured in the wavelength range of 350–750 nm with using a UV–visible spectrophotometer. The material components of the thin films were analyzed by using X-ray photoelectron spectroscopy (XPS).

3. Results and discussion

Figure 1 shows the sheet resistance of ITO thin film as a function of post-annealing temperature with/without buffer layers. In general, the sheet resistance of ITO thin film on corning glass decreases with annealing temperature caused by both the crystallization and the increased carrier concentration of the ITO thin film.[21–24] However, the sheet resistance of the ITO thin film deposited directly on the CSG is dramatically increased by the high-temperature (>200 °C) anneal process as shown in Fig. 1. From the results, we can expect that the out-diffusion of K^+ into the ITO thin film from the CSG leads to degrade the electrical properties of ITO thin films.

In order to suppress the potassium out-diffusion from the CSG, we inserted a SiO_2 and a Nb_2O_5 buffer layer between the ITO thin film and the CSG. In the case of the 55 nm SiO_2 buffer layer, though the sheet resistance of the ITO thin film is decreased from 155 to 135 Ω/sq by the post-annealing

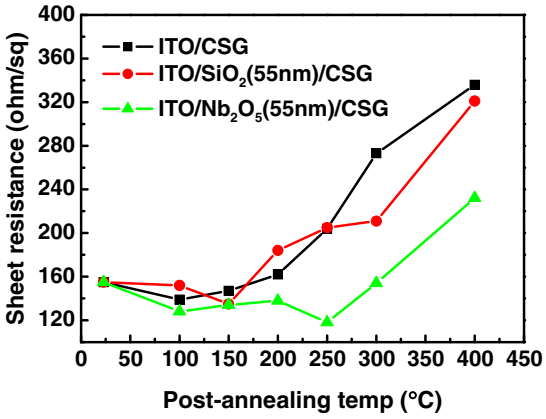

Fig. 1. (Color online) Sheet resistances of ITO thin films with SiO_2 and Nb_2O_5 buffer layers as a function of annealing temperature.

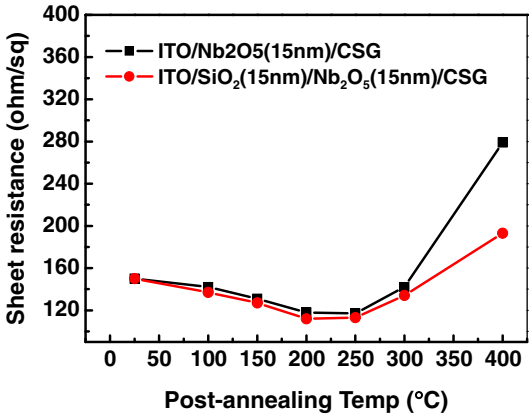

Fig. 2. (Color online) Sheet resistances of ITO/Nb_2O_5 (15 nm)/CSG and ITO/SiO_2 (15 nm)/Nb_2O_5 (15 nm)/CSG samples as a function of annealing temperature.

process at 150 °C, the sheet resistance is remarkably increased by the high-temperature (>200 °C) anneal process similar to the ITO thin film deposited directly on the CSG. However, in the case of 55 nm Nb_2O_5 buffer layer, the sheet resistance of the ITO thin film is not increased by the post-annealing process up to 300 °C. Moreover, the sheet resistance after post-annealing at 250 °C is as low as 118 Ω/sq. Therefore, those results indicate that the Nb_2O_5 layer is very effective to suppress the potassium out-diffusion from the CSG while the SiO_2 layer is less effective.

In order to demonstrate the effects of bulk and interface characteristics of buffer layers, we deposited a thinner Nb_2O_5 layer (15 nm) between ITO and CSG as shown in Fig. 2. The sheet resistance of the ITO/Nb_2O_5 (15 nm)/CSG sample does not increase after post-annealing process up to 300 °C with the lowest sheet resistance of 117 Ω/sq at the post-annealing temperature of 250 °C, which is quite similar to the ITO/Nb_2O_5 (55 nm)/CSG results. Therefore, we could conclude that the dominant factor for the suppression of the potassium out-diffusion is not the bulk but the interfaces of the Nb_2O_5 buffer layer. Additional reduction of the sheet resistance after 400 °C annealing is achieved by the insertion of a thin SiO_2 layer (15 nm) between the ITO and the Nb_2O_5 layer as shown in Fig. 2, which shows that the interface between SiO_2 and Nb_2O_5 would also play the role of diffusion barrier.

Table I. Material components in the surface region of various glasses analyzed by XPS measurements (in at. %).

	CSG	Soda lime glass	Corning glass
Si 2p	20.12	21.87	20.82
C 1s	9.58	11.4	10.92
K 2p	2.74	0.17	0
Rh 3d	0.73	0.61	0.2
Ca 2p	1.08	1.37	1.24
Sn 3d	2.86	0.15	0
O 1s	62.9	63.21	66.82
Na 1s		1.23	

Table II. Material components in the surface region of buffer layers after annealing analyzed by XPS measurement (in at. %).

	Nb_2O_5 (55 nm)/ CSG		SiO_2 (55 nm)/ CSG	SiO_2 (15 nm)/ Nb_2O_5 (15 nm)/CSG
	250 °C	400 °C	250 °C	250 °C
K 2p	0.13	1.88	1.42	0
C 1s	19.46	18.97	21.89	15.16
O 1s	59.44	59.44	56.02	60.18
Si 2p	0.66	0.64	20.53	26.65
Nb 3d	20.3	19.07	0.14	0

In order to confirm the suppression of the potassium out-diffusion by the Nb_2O_5 buffer layer, we analyzed the material elements in the surface region of various glasses and thin films by using XPS, which are summarized in Tables I and II, respectively. As shown in Table I, the CSG has non-negligible potassium ions (2.74 at. %) while the soda-lime and the corning glass have virtually no potassium ions as expected. In Table II, one can find that the surface regions of the Nb_2O_5 (55 nm)/CSG and the SiO_2 (15 nm)/Nb_2O_5 (15 nm)/CSG samples after 250 °C annealing have virtually no potassium ions (0–0.13 at. %), which indicates that the buffer layers (especially Nb_2O_5) really play the role of diffusion barrier of the K^+ and is consistent with the resistance data in Figs. 1 and 2. In the case of the SiO_2 (55 nm)/CSG after 250 °C annealing and the Nb_2O_5 (55 nm)/CSG sample after 400 °C annealing, the surfaces of the both samples have non-negligible atomic percent of K^+ (1.42–1.88 at. %), which is also consistent with the resistance data in Fig. 1. Figure 3 shows definite K 2p (K^+) XPS peaks (at around 293 eV) from the 250 °C annealing SiO_2 (55 nm)/CSG and the 400 °C annealing Nb_2O_5 (55 nm)/CSG samples.

The measured optical transmittances of ITO/SiO_2 (55 nm)/Nb_2O_5 (15 nm)/CSG and ITO/CSG samples are plotted in Fig. 4. The thicknesses of the SiO_2 (55 nm) and the Nb_2O_5 (15 nm) buffer layers are carefully chosen by index matching condition for the 30-nm-thick ITO layer.[25–29] In Fig. 4, the optical transmittances of the ITO/SiO_2 (55 nm)/Nb_2O_5 (15 nm)/CSG and the ITO/CSG are 88.1 and 82.0%, respectively, at the wavelength of 550 nm before 200 °C annealing. The dramatic increase of the transmittance in the ITO/SiO_2 (55 nm)/Nb_2O_5 (15 nm)/CSG sample is due to the index matching effect by the SiO_2 (55 nm)/Nb_2O_5

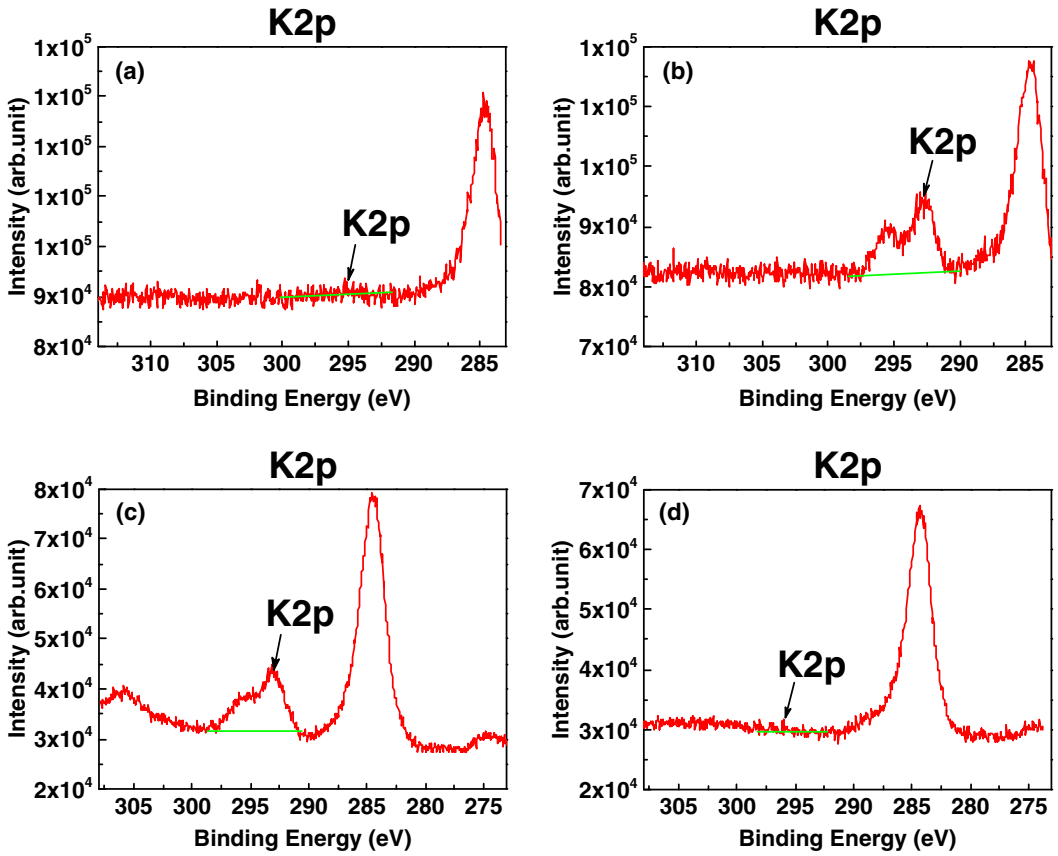

Fig. 3. (Color online) XPS peaks of Nb_2O_5 (55 nm)/CSG after 250 °C annealing (a), 400 °C annealing (b), SiO_2 (55 nm)/CSG after 250 °C annealing (c), and SiO_2 (15 nm)/Nb_2O_5 (15 nm)/CSG after 250 °C annealing (d).

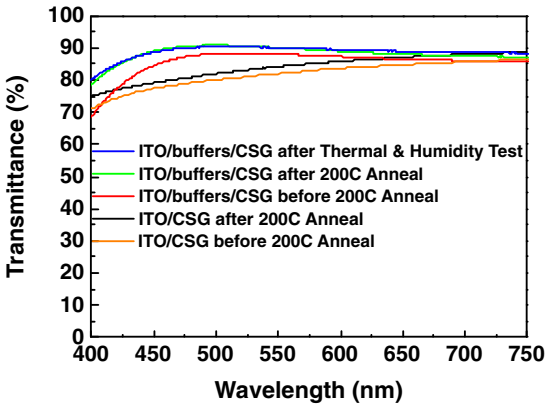

Fig. 4. (Color online) Optical transmittance of ITO/CSG before 200 °C anneal (orange), after 200 °C anneal (black), ITO/SiO_2 (55 nm)/Nb_2O_5 (15 nm)/CSG before 200 °C anneal (red), after 200 °C anneal (green), and after thermal and humidity reliability tests (blue).

(15 nm) buffer layers.[29] In the case of the 200 °C annealing, the optical transmittances of both samples are slightly increased by about 2%, which is due to the crystallization of the ITO. In that case, the out-diffusion of potassium ions does not seem to affect the optical characteristic of the ITO thin film, which is possibly due to the fact that the optical constants of semiconductors are mainly related with band and crystal structures. The optical transmittance of 90.1% is achieved in the ITO/SiO_2 (55 nm)/Nb_2O_5 (15 nm)/CSG sample at a wavelength of 550 nm as shown in Fig. 4. We conducted a thermal and a humidity stress test of the annealed ITO/SiO_2 (55 nm)/Nb_2O_5 (15 nm)/CSG sample for 20 and 200 h, respectively. The thermal stress test was conducted at 40 and 85 °C for 30 min each with 20 times. The humidity stress test was conducted at 65 °C with 95% humidity. As shown in Fig. 4, the optical transmittance of the ITO thin film does not change much after the humidity and thermal stress tests. Moreover, the change of the sheet resistance after the stress tests is less than 1 Ω/sq (not shown here). Therefore, we can conclude that the electrical and optical properties of the ITO/SiO_2/Nb_2O_5/CSG structure are relatively stable under humid and high temperature environment.

4. Conclusions

In this study, we have investigated the effects of buffer layers such as SiO_2 and Nb_2O_5 between the ITO layer and the CSG substrate to suppress the out-diffusion of K^+ from the CSG. From electrical and XPS analyses, we have found that the Nb_2O_5 buffer layer (especially its interfaces) would play the role of diffusion barrier of the K^+ from the CSG. As a result, the protected and index-matched ITO thin film with sheet resistance less than 120 Ω/sq and transmittance higher than 90% at the wavelength of 550 nm has been achieved after 200 °C anneal process. Moreover, the optical and electrical properties of the ITO thin film show virtually no change under humidity and thermal stress tests. Our result can be applied to large-size and highly transparent DPW-TSPs.

Acknowledgements

This work was supported by R&D project of MKE/KEIT (10039263, Development of window-unified 30″ touch sensor).

1) S. K. Kim, W. Choi, W. J. Rim, Y. T. Chun, H. S. Shim, H. J. Kwon, J. S. Kim, I. S. Kee, S. C. Kim, S. Y. Lee, and J. S. Park, IEEE Trans. Electron Devices **58**, 10 (2011).
2) T. H. Hwang, W. H. Cui, I. S. Yang, and O. K. Kwon, IEEE Trans. Consum. Electron. **56**, 1115 (2010).
3) J. A. Pickering, Int. J. Man–Mach. Stud. **25**, 249 (1986).
4) S.-Z. Peng, S.-C. Huang, S.-H. Huang, Y.-N. Chu, W.-T. Tseng, and H.-T. Yu, SID Symp. Dig. Tech. Pap. **40**, 567 (2009).
5) M. R. Bhalla and A. V. Bhalla, Int. J. Comput. Appl. **6** [8], 12 (2010).
6) S. J. Park, 6th Display Bank, 2010, p. 1.
7) H. W. Lehmann and R. Widner, Thin Solid Films **27**, 359 (1975).
8) J. Machet, J. Guille, P. Saulnier, and S. Robert, Thin Solid Films **80**, 149 (1981).
9) J. Kane and H. P. Schweizer, Thin Solid Films **29**, 155 (1975).
10) J. L. Yao, S. Hao, and J. S. Wilkinson, Thin Solid Films **189**, 227 (1990).
11) A. K. Kulkarni and S. A. Knickerbocker, Thin Solid Films **220**, 321 (1992).
12) C. H. Hong, Y. J. Jo, and J. S. Kwak, J. Ceram. Process. Res. **12**, s138 (2011).
13) C. H. Hong, S. M. Wie, M. J. Park, and J. S. Kwak, J. Nanosci. Nanotechnol. **13**, 5420 (2013).
14) R. Gy, Mater. Sci. Eng. B **149**, 159 (2008).
15) A. L. Zijlstra and A. J. Burrggraaf, J. Non-Cryst. Solids **1**, 163 (1969).
16) R. Y. Tsai, F. C. Ho, and M. Y. Hua, Opt. Eng. **36**, 2335 (1997).
17) J. S. Hong, B. R. Rhee, H. M. Kim, K. C. Je, T. J. Kang, and J. S. Ahn, Thin Solid Films **467**, 158 (2004).
18) J. C. Imbert, L. De Poucques, C. B. Laporte, J. Bretagne, M. C. Hugon, D. Pagnon, P. Pitach, L. T. Gay, and M. Touzeau, Thin Solid Films **516**, 4700 (2008).
19) I. H. Yang, Y. J. Lee, J. N. Jang, and M. P. Hong, Thin Solid Films **517**, 4165 (2009).
20) K. H. Lee and H. W. Jang, J. Appl. Phys. **95**, 586 (2004).
21) W. G. Haines, J. Appl. Phys. **49**, 304 (1978).
22) H. Morikawa and M. Fujita, Thin Solid Films **339**, 309 (1999).
23) H. C. Lee and O. O. Park, Vacuum **75**, 275 (2004).
24) N. Balasubramanian and A. Subrahmanyam, J. Phys. D **22**, 206 (1989).
25) M. Born and E. Wolf, *Principles of Optics* (Cambridge University Press, Cambridge, U.K., 1999) 7th ed.
26) J. Q. Xi, M. F. Schubert, J. K. Kim, E. Fred Schubert, M. Chen, S. Y. Lin, W. Liu, and J. A. Smart, Nat. Photonics **1**, 176 (2007).
27) X. Yan, F. W. Mont, D. J. Poxson, M. F. Schubert, J. K. Kim, J. H. Cho, and E. Fred Schubert, Jpn. J. Appl. Phys. **48**, 120203 (2009).
28) C. H. Hong, J. H. Shin, K. H. Kim, N. M. Park, B. S. Kim, B. K. Ju, and W. S. Cheong, 2nd Int. Conf. Electronic Materials and Nanotechnology for Green Environment, 2012, p. 57.
29) C. H. Hong, J. H. Shin, B. K. Ju, K. H. Kim, N. M. Park, B. S. Kim, and W. S. Cheong, J. Nanosci. Nanotechnol. **13**, 7756 (2013).